

Transcriptome Profiling of the Abdominal Skin of *Larimichthys crocea* in Light Stress

HAN Zhaofang¹, LV Changhuan¹, XIAO Shijun¹, YE Kun¹, ZHANG Dongling¹, TSAI Huai Jen², and WANG Zhiyong^{1,*}

1) Key Laboratory of Healthy Mariculture for the East China Sea of Ministry of Agriculture, Fisheries College, Jimei University, Xiamen 361021, China

2) Institute of Biomedical Sciences, Mackay Medical College, New Taipei City, Taiwan, China

(Received December 2, 2016; revised April 24, 2017; accepted September 4, 2017)

© Ocean University of China, Science Press and Springer-Verlag GmbH Germany 2018

Abstract Large yellow croaker (*Larimichthys crocea*), one of the most important marine fish species in China, can change its abdominal skin color when it is shifted from light to dark or from dark to light, providing us an opportunity of investigating the molecular responding mechanism of teleost in light stress. The gene expression profile of fish under light stress is rarely documented. In this research, the transcriptome profiles of the abdominal skin of *L. crocea* exposed to light or dark for 0 h, 0.5 h and 2 h were produced by next-generation sequencing (NGS). The cluster results demonstrated that stress period, rather than light intensity (e.g., light or dark), is the major influencing factor. Differently expressed genes (DEGs) were identified between 0 h and 0.5 h groups, between 0 h and 2 h groups, between 0.5 h light and 0.5 h dark, and between 2 h light and 2 h dark, respectively. The gene ontology (GO) and Kyoto Encyclopedia of Genes and Genomes (KEGG) annotation revealed that the genes relating to immunity, energy metabolism, and cytoskeletal protein binding were significantly enriched. The detailed analysis of transcriptome profiles also revealed regular gene expression trends, indicating that the elaborate gene regulation networks underlined the molecular responses of the fish to light stress. This transcriptome analysis suggested that systematic and complicated regulatory cascades were functionally activated in response to external stress, and coloration change caused by light stress was mainly attributed to the change in the density of chromatophores for *L. crocea*. This study also provided valuable information for skin coloration or light stress research on other marine fish species.

Key words skin transcriptome; light stress; coloration change; *Larimichthys crocea*; gene expression

1 Introduction

In the wild and aquaculture conditions, marine fish expose to variable environmental stresses (Fu *et al.*, 2014). In recent years, fish adaptation and response to several important external stresses, such as temperature (Smith *et al.*, 2013), salinity (Larsen *et al.*, 2012) and hypoxia (Ao *et al.*, 2015), were investigated, providing us the knowledge of molecular and physiological changes of fish upon they meet these stresses. The sequencing-based investigations demonstrated that these stresses to aquatic organisms can affect physiological functions, including metabolism, immunity, growth and development (Schartl *et al.*, 2013). In fish aquaculture pond, light could influence circadian rhythms of spawning and feeding, which has important effects on breeding and growth (Blanco-Vives, and Sánchez-Vázquez, 2009). Additionally, we noticed that light intensity (e.g., light or dark) can cause fish coloration changes.

The large yellow croaker, *Larimichthys crocea*, is a temperate-water migratory fish that belongs to the order of Perciformes and the family of Sciaenidae (Xiao *et al.*, 2015). It is a commercially important marine species in China and East Asian countries owing to its high nutrition and delicate flavor. In recent decades, *L. crocea* aquaculture ranks the top in production among all net-caged marine fish species in China (Liu *et al.*, 2014; Liu *et al.*, 2013). The skin color correlates with price of the fish; the price of yellow individuals is about 3 times higher than yellowish ones. Up to date, the basic researches around the genetic improvement of the growth and disease resistance of *L. crocea* have been performed (Ye *et al.*, 2014; Mu *et al.*, 2010; Dong *et al.*, 2016). *L. crocea* exhibits behavioral and physiological sensitivities to sound, lights and other environments (Su *et al.*, 2007; Zhou *et al.*, 2011). According to the previous reports, *L. crocea* can quickly and robustly respond to hypoxia in its brain (Gu and Xu, 2011). A lot of mucus would be secreted from the skin when it is exposed to air (Su *et al.*, 2007). Meanwhile, the skin changes color when the light is dim. These traits make *L. crocea* a suitable experimental animal to

* Corresponding author. E-mail: zywang@jmu.edu.cn

investigate the molecular response of teleost to environmental changes. Although the proteomic changes in blood and mucus of hypoxia-treated *L. crocea* have been reported (Ao *et al.*, 2015; Gu *et al.*, 2011), the skin transcriptome profile of this species in light stress is largely unknown.

With the advances of high-throughput next-generation sequencing (NGS) technologies, RNA-seq is particularly suitable for quantifying transcript abundance in complex conditions. To study gene expression profile and identify possible driver genes in response to light stress, two groups of large yellow croakers were separately exposed to light for 0.5 h and 2 h; two groups were respectively exposed to dark for 0.5 h and 2 h; two groups were firstly exposed to dark for 0.5 h and 2 h and then treated with light for 5 min; while the group without being exposed to light or light was control. We sequenced and analyzed the transcriptome of the abdominal skin of *L. crocea*. All differently expressed genes (DEGs) were grouped in GO enrichments and KEGG pathways for functional annotation. Our findings indicated that the density of chromatophores changes induced by light might lead to skin coloration change in *L. crocea*, while genes with steady expression trends involved in the systematic and complicated molecular signal pathways could play a key role in responding to the light stress.

2 Materials and Methods

2.1 Ethics Statement

All experimental procedures were conducted in conformity with institutional guidelines for the care and use

of laboratory animals, and protocols were approved by the Animal Care and Use Committee of Fisheries College of Jimei University.

2.2 Sample Collection and Stressing Experiment

Totally 140 *L. crocea* (90–100 g) individuals were collected from a mariculture farm in Ningde, Fujian Province, China. They were acclimated in aerated seawater at about 23°C for seven days. The pilot experiment indicated that the skin coloration of *L. crocea* could change from yellowish to golden yellow when they were exposed to the dark for 0.5 h, and remain stable golden if being kept in dark. However, the coloration would rapidly recover to normal when it was transferred to light condition (Fig.1). According to that, stress experiments were conducted with the following methods. All 140 selected individuals were transferred to laboratory and separated equally into seven groups, 20 each. For control (0h), abdominal skins including epidermis and dermis (approximate size of 1 cm²) were directly collected, and immediately frozen in liquid nitrogen. And the other six groups were respectively stressed for 0.5 h and 2 h in a tank with three treatments: exposed to daylight lamp (2500Lm) (light groups); covered with a light-tight cloth in dark (dark groups); and firstly cultured in dark and then recovered in light for 5 min (recovery groups). Before skin collections, all organisms were rightly dipped with anesthetic. Then the scales were removed with tweezers and the muscle adhering to the skin was wiped off using a scalpel. A total of 140 abdominal skin samples were dissected, directly frozen in liquid nitrogen, and stored in a –80°C freezer for RNA collection.

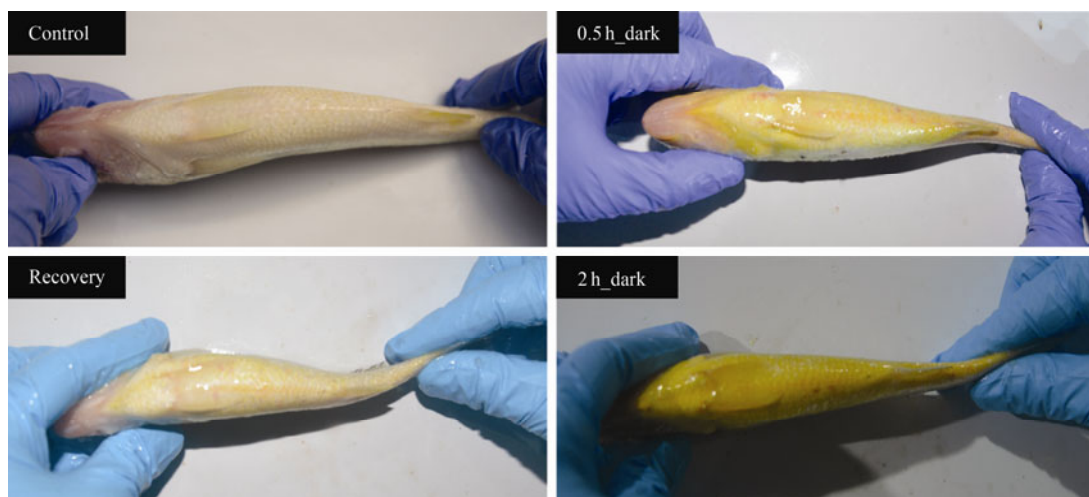


Fig.1 The abdominal skin coloration of *L. crocea* changed in treatments of control (0h), 0.5h in dark, 2h in dark and recovery from dark to light.

2.3 RNA Extraction and Sequencing

Total RNA was extracted from the abdominal skin of each fish each group with Trizol Reagent (Invitrogen, CA, USA), and then pooled together with equal amounts each group. Purified RNA samples were detected with 260 nm/280 nm ranging from 2.0 to 2.2 and RIN ranging from

7.4 to 8.4 using Nanodrop ND-1000 spectrophotometer (LabTech, Ringmer, UK) and Agilent 2100 Bioanalyzer (Agilent Technologies, Palo Alto, CA), respectively. The high-quality RNA samples were used to construct RNA libraries using the TruSeq RNA Sample Prep Kit (Illumina, CA, USA). The libraries were sequenced on the HiSeq 2000 platform (Illumina, CA, USA) with 100 bp

sequenced from both ends (paired-end).

2.4 Gene Expression Estimation and Differentially Expressed Gene Analysis

To retain high-quality reads for gene expression estimation, raw reads were trimmed with HTQC toolkit (Yang *et al.*, 2013) by removing four kinds of low-quality reads: 1) adaptor contaminated sequences; 2) with unknown bases ('N') greater than 5%; 3) with five continuous low-quality bases at the 3'-end (Q-score < 20); 4) shorter than 50 bp after trimming. The filtered high-quality reads were mapped to *L. crocea* genome (Ao *et al.*, 2015) using Tophat software with default parameters (Trapnell *et al.*, 2012). To normalize and estimate the abundance each transcript, FPKM (Fragment Per Kilo base per Million) scores were calculated with Cufflinks (Tu *et al.*, 2012). We compared treatment groups with control and light groups with dark groups to identify DEGs induced by stress duration and light stress using Cuffdiff software (Trapnell *et al.*, 2013). The thresholds of significantly different expression were set at P -value < 0.05 and fold change (FC) > 2. Meanwhile, edgeR (Robinson *et al.*, 2010) was also used to identify DEGs based on previously reported gene annotation of *L. crocea* (Ao *et al.*, 2015). WEGO (Ye *et al.*, 2006) was adopted in Gene Ontology (GO) annotation analysis of the DEGs. Furthermore, enrichment analyses in GO terms and Kyoto Encyclopedia of Genes and Genomes (KEGG) pathways were performed with custom scripts.

2.5 qRT-PCR Validation

Twelve genes at different expression levels related to functional biological process were selected in qRT-PCR validation. As a result, 9 out of 12 genes (75%) were successfully amplified. These 9 candidate genes were quantified, and the libraries of 0.5 h and 2 h treatments were compared with that of control (0 h), respectively. Total RNA were extracted from abdominal skin with Trizol Reagent (Invitrogen, Carlsbad, CA) according to the manufacturer's instructions. The first strand cDNA was synthesized using GoScript™ Reverse Transcription System kit (Promega) following the manufacturer's protocol. The qRT-PCR was performed on StepOnePlus thermocycler (Applied Biosystems) using SuperReal PreMix Plus SYBR Green I (Tiangen Biotech, Beijing, China). The primers of target genes used in qRT-PCR were designed using Primer 5.0 software and listed in Table 1. β -actin, served as the internal control, was amplified with β -actin-F and R. The amplifications were carried out in a total volume of 20 μ L containing 6.8 μ L of 1:100 diluted cDNA, 10 μ L 2 \times SuperReal PreMix Plus SYBR Green I, 2 μ L 50 \times ROX Reference Dye and 0.6 μ L of each primer (10 μ mol μ L⁻¹). The amplification program was as follows: 95°C for 15 min, 40 cycles with 95°C for 15 s and 60°C for 1 min, followed by a dissociation stage to verify the specificity of PCR products. All samples were tested in quadruplicate. The relative expression of each target gene was determined by comparative threshold cycle method ($2^{-\Delta\Delta C_t}$).

Table 1 Primers for amplification of selected differently expressed genes (DGE) and internal control genes

Annotation	Forward (5'-3')	Reverse (5'-3')
Activating transcription factor 3 (ATF3)	CCAGCGAGGAAGCGAAACA	AAGTCGTCCAGGGTGAGCGT
Calreticulin 3b (CALR3b)	AGTTCTACGGAGATGCTGAGGC	TGGATGACCAGGGGCTTTC
Heat shock 70kDa protein 5 (HSPA5)	AGGCTCATGGAGATGCTGC	GGACTTTGGGTTTTCCGCTAT
Heat shock protein 8 (HSPA8)	GATTTCTCAACGGCAGGGAG	TTTAGCGGGGATGGTGGTG
Claudin e (CLDNE)	ATCGTTGCTGCCTTTGGG	CAGACGGGGATAAAGGATGAGA
Actin, alpha, cardiac muscle 1 (ACTC1)	GAACCCCAAAGCCAACAGG	TCACCAGAGTCCAGCACGATAC
Leukocyte cell-derived chemotaxin 2 (LECT2)	AGCCAGACGGCAAACCAGA	CGTAGAACAACCTGAAGCACAGAC
Major histocompatibility complex I (MHC-I)	TTTGTTGCTGTTGGGATAGTTG	TCCAGTCTGTTTCGGTTCTT
Ribonucleotide reductase M1 (RRM1)	TCTACGGCTGGAAGTTGGG	TCTCCTCTCGCTCTTGTT

3 Results

3.1 Raw Sequencing Reads and Quality Statistics

To understand the change of gene expression in response to light stress, the seven libraries (7 groups) constructed from skin of *L. crocea* were sequenced in the HiSeq 2000 platform (Illumina). As shown in Table 2, a

total of 129.6 million of raw reads were generated, and an average of 15.3, 18.5 and 19.6 million reads were obtained from libraries of the control (0 h), 0.5 h duration and 2 h duration group, respectively. After reads filtering, a total of 128.9 million (99.5% of raw reads) clean reads were obtained. The percentages of Q30 bases are more than 95% for all samples, ensuring good results of the following reads alignment and analysis. We noticed that

Table 2 Statistic summary of the transcriptomic data generated from *L. crocea*

Treatment	Library	Raw reads	Clean reads	Average reads length (bp)	Q30 (%)	GC (%)
Control (0 h)	Control	15273653	15192467	89.71	95.21	48.0
	0.5 h_light	15536378	15457027	90.12	95.14	49.5
0.5 h-treatment	0.5 h_dark	18893105	18797645	90.10	95.19	48.5
	0.5 h_recovery	21133364	21046245	90.09	95.82	49.0
	2 h_light	21377309	21275133	90.48	95.33	49.0
2 h-treatment	2 h_dark	19972523	19891992	90.50	95.87	49.0
	2 h_recovery	17385944	17304477	90.16	95.79	49.0

the clean reads with an average length of 90bp (<100bp) because of the end-trimming of low-quality bases. Raw sequencing data were deposited in the NCBI Sequence Read Archive (SRA) under Project Accession PRJNA-303096.

3.2 Sample Clustering and Differential Expression Genes Analysis

The high-quality reads were aligned to the draft reference genome of the large yellow croaker, while 48.07% reads were mapped and 40.09% reads were uniquely mapped, and a total of 95913 transcripts were assembled. For gene expression clusters, samples with the same duration time (0.5 h or 2 h) rather than same treatment (light, dark and recovery) were grouped together (Fig.2), which suggested that stress durations (0.5 h and 2 h) rather than light or dark were the principal stress factor.

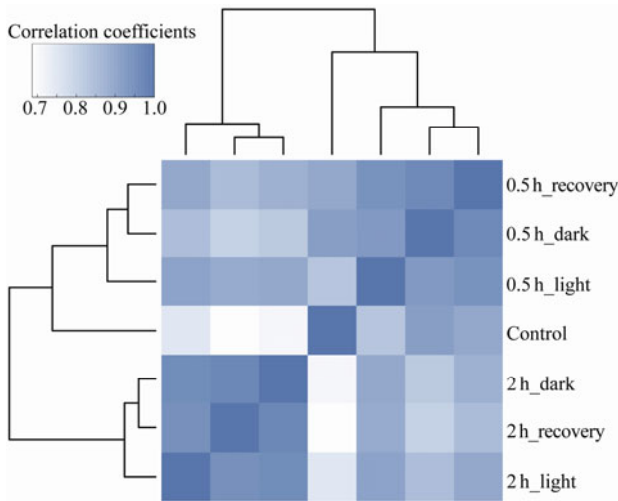


Fig.2 Gene expression correlation analysis of *L. crocea* under the light stress. The color scheme represents for correlation coefficients among samples.

To identify key genes responding to duration stress, differentially expressed genes were analyzed between the control and 0.5h-treatment group (0h–0.5h), as well as between the control and 2h-treatment group (0h–2h). For the treatment duration comparisons, 758 (0h–0.5h) and 1912 (0h–2h) DEGs were identified. Among the DEGs identified with Cuffdiff, 397 genes were up-regulated and 361 genes were down-regulated in the 0h–0.5h comparison, and 1016 genes were up-regulated and 896 genes were down-regulated in the 0h–2h comparison (Fig.3(B)). More genes were up-regulated, suggesting a large number of genes were activated in the response of duration stress. These genes, showed different expression levels after stress, may play important roles in physiological processes associated with light duration stress. As shown in Fig.3(A), 496 (0h–0.5h) and 1515 (0h–2h) DEGs were detected by edgeR. A total of 241 and 995 DEGs were detected by both methods in the comparisons of 0h–0.5h and 0h–2h, respectively. To evaluate the consistence of the two methods, Fisher exact test (Upton, 1992) was performed to calculate the significance of the number of

the shared DEGs. We found that the shared DEGs identified by Cuffdiff and edgeR were extremely significant for both comparisons ($P < 2 \times 10^{-6}$ in both cases), indicating that the DEGs identified in the two programs were generally consistent with each other. With genome sequence and gene structure information (exon and intron coordinate) in Cuffdiff, alternative splicing and exon usage analysis can be conducted (Hooper, 2014). Therefore, DEGs detected by Cuffdiff were chosen for further annotations and pathway analysis.

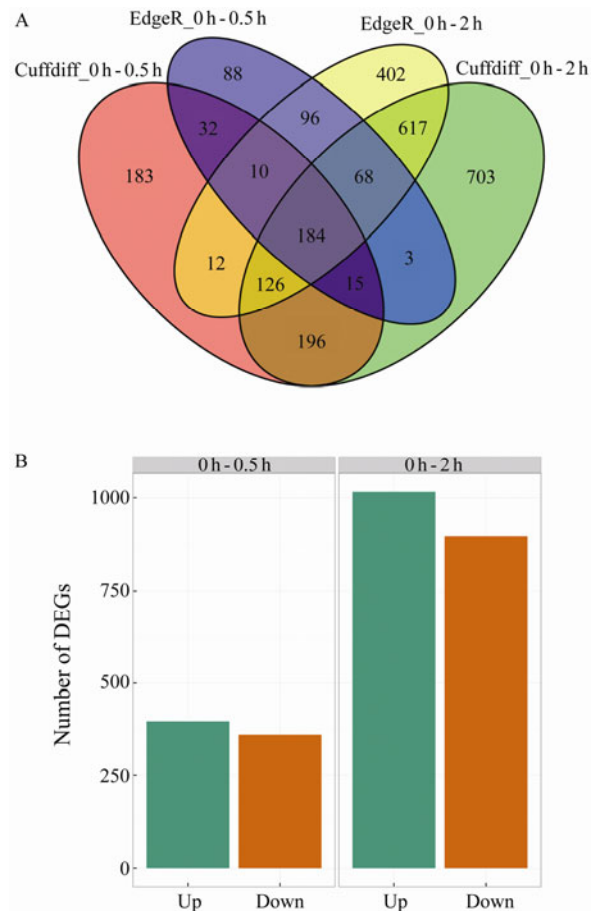


Fig.3 DEGs identification during the light stress. (A) Venn diagram of DEGs detected by Cuffdiff and edgeR. Intersections of circles indicate stress-responsive DEGs among different time point comparisons or different methods. (B) The number of up-/down-regulated DEGs identified by Cuffdiff.

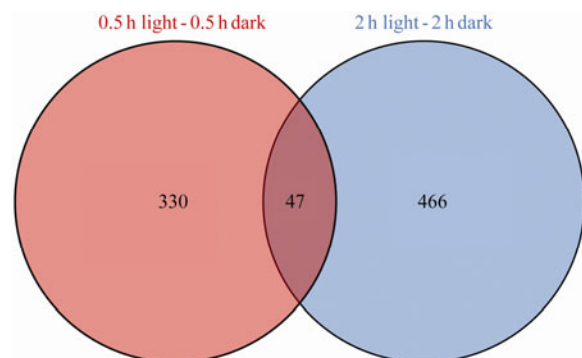


Fig.4 Venn plots of DEGs in comparisons between light and dark with same duration (0.5 h and 2 h).

The further sample comparisons of light with dark in same duration investigated 377 (0.5 h) and 513 (2 h) DEGs, respectively (Fig.4). And 47 DEGs were shared in the above-mentioned two comparisons, which likely caused by the light or dark treatment.

3.3 GO and KEGG Pathway Enrichment Analysis

DEGs that were identified in the comparisons of 0 h–0.5 h and 0 h–2 h were used for GO enrichment analysis. In the 0 h–0.5 h comparison, 610 of 758 (80.5%) unigenes were classified into three major functional categories (*i.e.*, biological process, cellular component and molecular functions), and 237 subcategory terms, including 160 (67.5%) BP categories, 30 (12.7%) CC categories and 47 (19.8%) MF categories. In the 0 h–2 h comparison, 1523 of 1912 (79.7%) unigenes were annotated into 287 sub-

categories, including 191 (66.5%) BP categories, 41 (14.3%) CC categories and 55 (19.2%) MF categories. The detailed annotations for each category were depicted in Fig.5. Cellular process (GO:0009987) and metabolic process (GO:0008152) were the most enriched components out of BP terms; organelle (GO:0043226) and macromolecular complex (GO:0032991) were the most common terms in CC terms; while binding (GO:0005488) and cellular part (GO:0044464) were the top two terms in MF category. Within each of the three categories, some genes were assigned to subcategories of immune response (GO:0002376), responding to stimulus (GO:0050896) and structural molecule activity (GO:0005198). These immune-relevant and structure-sensitive genes might play key roles in responding to stress duration and other environment stresses.

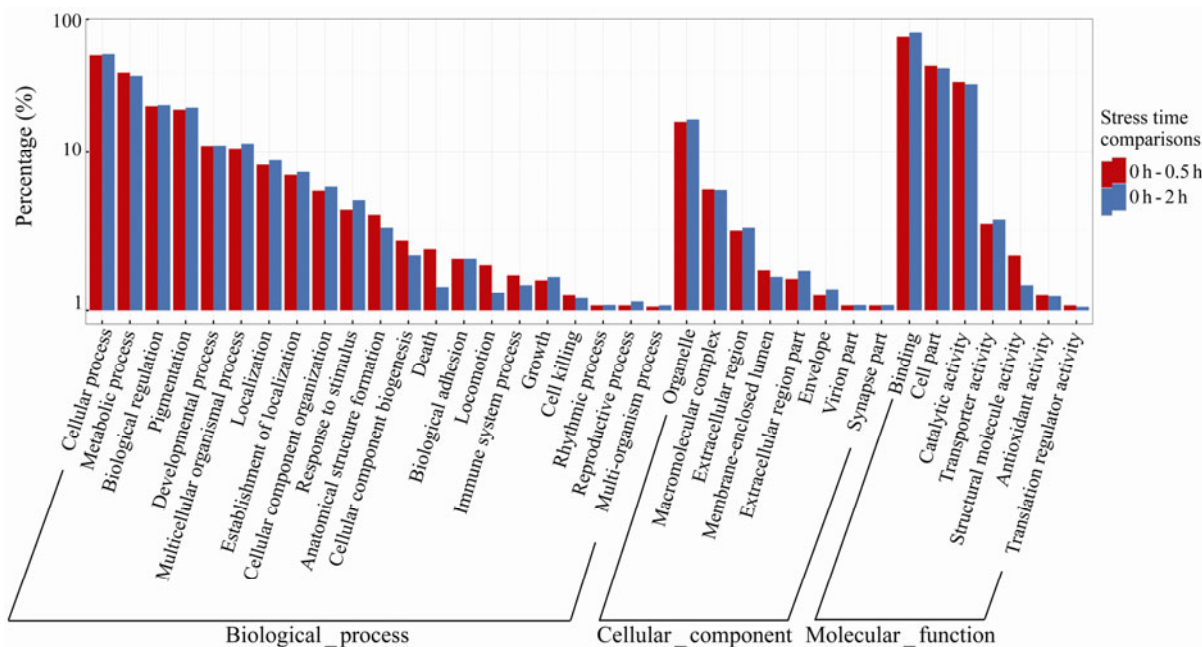


Fig.5 Function of DEGs in *L. crocea* in response to stress based on Gene Ontology distribution. GO subcategories are on the X-axis. Y-axis represents the percentage of genes in total DEGs. Red color represents the comparison between the control sample and 0.5 h-stress samples. Blue color represents the comparison between the control sample and 2 h-stress samples.

In addition, several function categories were significantly enriched among DEGs. For the stress duration analysis, significantly enriched DEGs of 0 h–0.5 h comparison were mainly related to cytoskeletal protein, immunity and cell apoptosis. Cytoskeletal protein related categories were detected in GO enrichments including cartilage morphogenesis (GO:0060536), actin binding (GO:0003779) and cytoskeletal protein binding (GO:0008092) (Table 3). The immune-relevant items were identified in KEGG metabolism pathways including phagosome, leukocyte transendothelial migration, lysosome, pathogenic *Escherichia coli* infection and Shigellosis (Table 4). Regulation of apoptotic process (GO:0042981) and DNA replication can be classified as cell apoptosis. Compared with duration of 0 h–0.5 h, most items of DEGs identified in 0 h–2 h duration comparison were identical

except for energy metabolism, which was identified in GO enrichments (*e.g.*, oxoacid metabolic process (GO:0043436) and cellular modified amino acid metabolic process (GO:0006575)) and KEGG pathway (*e.g.*, Fructose and mannose metabolism). The identical categories of cytoskeletal protein might be resulted from light or dark stress. Many immunity and cell apoptosis related categories were enriched can aid to avoid inflammatory injury in fish. Energy metabolism category specially found in 2 h stress duration can help the fish maintain energy balance during the stress processing. Besides, other metabolisms such as glutathione metabolism, arrhythmogenic right ventricular cardiomyopathy and GnRH signaling pathway were also identified in the enrichments.

Furthermore, the light and dark samples of identical duration (0.5 h or 2 h) were compared to develop DEGs

just corresponding to light or dark. As shown in Table 5, enrichments of 47 shared DEGs were mainly composed of cytoskeletal protein (e.g., cytoskeleton (GO:0005856)), muscle cell development (GO:0055001), skeletal muscle tissue development (GO:0007519) and regulation of actin cytoskeleton (ko04810) and pigmentation (e.g.,

eye pigmentation (GO:0048069) and developmental pigmentation (GO:0048066)). Therefore, we speculate that the reason for the coloration change of abdominal skin might be that dark stress can cause the cytoskeletal change, thus leads to the change in the density of chromatophores.

Table 3 Significant GO enrichments with significantly annotated DEGs for comparisons of the control and 0.5 h-treatment group (0h–0.5 h) and the control and 2h-treatment group (0h–2 h)

Comparison	GO ID	GO term description	Counts	Sizes	FDR
0h□0.5h	GO:0060536	Cartilage morphogenesis	7	14	0.000
	GO:0060788	Ectodermal placode formation	6	17	0.010
	GO:0048708	Astrocyte differentiation	3	3	0.015
	GO:0043049	Otic placode formation	5	12	0.017
	GO:0030916	Otic vesicle formation	5	14	0.039
	GO:0042981	Regulation of apoptotic process	18	164	0.046
	GO:0043067	Regulation of programmed cell death	18	166	0.050
	GO:0003779	Actin binding	21	215	0.015
	GO:0008092	Cytoskeletal protein binding	29	367	0.040
	GO:0043436	Oxoacid metabolic process	70	361	0.009
	GO:0019752	Carboxylic acid metabolic process	68	353	0.014
	GO:0043207	Response to external biotic stimulus	22	76	0.017
	GO:0007049	Cell cycle	62	316	0.017
	GO:0000188	Inactivation of MAPK activity	6	8	0.020
0h□2h	GO:0043407	Negative regulation of MAP kinase activity	7	11	0.022
	GO:0042074	Cell migration involved in gastrulation	19	64	0.036
	GO:0006575	Cellular modified amino acid metabolic process	18	60	0.046
	GO:0005856	Cytoskeleton	100	603	0.005
	GO:0000796	Condensin complex	4	4	0.008
	GO:0043292	Contractile fiber	11	29	0.010
	GO:0015629	Actin cytoskeleton	34	170	0.038
	GO:0005509	Calcium ion binding	130	788	0.005
	GO:0016755	Transferase activity, transferring amino-acyl groups	11	29	0.022

Notes: Counts indicate DEGs clustered into the GO terms; sizes indicate all unigenes associated with the GO terms. FDR represents for false discovery rate.

Table 4 The top 10 KEGG pathways with significantly annotated DEGs for the 0h–0.5 h comparison group and the 0h–2 h comparison group

Comparison	KEGG ID	Pathway description	Counts	Sizes	FDR
0h–0.5 h	ko04380	Osteoclast differentiation	18	151	0.005
	ko04145	Phagosome	20	182	0.007
	ko05130	Pathogenic Escherichia coli infection	11	69	0.007
	ko04670	Leukocyte transendothelial migration	19	187	0.022
	ko05412	Arrhythmogenic right ventricular cardiomyopathy	14	131	0.050
	ko04142	Lysosome	15	146	0.050
	ko04912	GnRH signaling pathway	13	128	0.108
	ko00480	Glutathione metabolism	6	41	0.148
	ko03030	DNA replication	6	42	0.153
	ko05131	Shigellosis	9	83	0.167
0h–2 h	ko04670	Leukocyte transendothelial migration	44	187	0.002
	ko04380	Osteoclast differentiation	35	151	0.012
	ko00480	Glutathione metabolism	13	41	0.047
	ko04612	Antigen processing and presentation	17	61	0.047
	ko04141	Protein processing in endoplasmic reticulum	40	197	0.050
	ko00330	Arginine and proline metabolism	15	55	0.096
	ko00051	Fructose and mannose metabolism	16	63	0.148
	ko03030	DNA replication	12	42	0.148
	ko04110	Cell cycle	29	143	0.217
	ko04145	Phagosome	35	182	0.236

Table 5 Significant GO and KEGG enrichments of the 47 shared DEGs identified from comparisons between 0.5 h-light and 0.5h-dark group and between 2 h-light and 2-dark

Class	Category ID	Description	Counts	Sizes	FDR
GO	GO:0048069	Eye pigmentation	1	1	0.002
	GO:0003875	ADP-ribosylarginine hydrolase activity	1	2	0.003
	GO:0004979	Beta-endorphin receptor activity	1	2	0.003
	GO:0016595	Glutamate binding	1	2	0.003
	GO:0042412	Taurine biosynthetic process	1	3	0.005
	GO:0005856	Cytoskeleton	3	238	0.008
	GO:0055001	Muscle cell development	1	5	0.009
	GO:0005523	Tropomyosin binding	1	7	0.012
	GO:0048066	Developmental pigmentation	1	8	0.014
	GO:1900052	Regulation of retinoic acid biosynthetic process	1	8	0.014
	GO:0003823	Antigen binding	1	10	0.017
	GO:0004129	Cytochrome-c oxidase activity	1	13	0.022
	GO:0016192	Vesicle-mediated transport	2	146	0.026
	GO:0004930	G-protein coupled receptor activity	4	676	0.028
	GO:0007519	Skeletal muscle tissue development	1	18	0.031
	GO:0007186	G-protein coupled receptor signaling pathway	4	760	0.041
	GO:0005575	Cellular_component	7	1929	0.044
	GO:0005509	Calcium ion binding	4	788	0.046
KEGG	ko04670	Leukocyte transendothelial migration	4	187	0.003
	ko04530	Tight junction	4	233	0.004
	ko05416	Viral myocarditis	3	117	0.004
	ko04510	Focal adhesion	4	320	0.006
	ko04810	Regulation of actin cytoskeleton	3	287	0.031
	ko05412	Arrhythmogenic right ventricular cardiomyopathy (ARVC)	2	131	0.036
	ko00603	Glycosphingolipid biosynthesis - globo series	1	14	0.036
	ko00604	Glycosphingolipid biosynthesis - ganglio series	1	20	0.041
	ko04145	Phagosome	2	182	0.045

3.4 Gene Expression Trend with Light Duration

Our experiments were designed to identify DEGs under light stress for different durations, which provided us a good chance to analyze gene expression trends associated with the stress duration. We clustered DEGs by their normalized expression levels (FPKM values) in Fig.6. All regulated genes were grouped into 14 clusters by their expression profiles, as shown by color bars besides the gene expression heat map (Fig.6). Eight out of fourteen expression trends were highlighted as subsets from 'a' to 'h'. Regular gene expression trends including increasing and descending, were observed in the majority of the clusters. Detailed GO annotation analysis suggested that the genes clustered by expression also enriched in similar biological functions. The most significant enriched pathways in the increasing trends of b, c, f and g were related to fatty acid metabolic process, response to lipid, inactivation of MAPK activity, and intermediate filament cytoskeleton organization, respectively; while the functions of genes in the descending trends of d and e were enriched in response to external stimulus and oxidoreductase activity, respectively. The regular trend of transcript abundances revealed systematic and complicated regulatory cascades in responding to light stress.

3.5 Validation of Gene Expression Levels

Nine out of twelve genes related with immune systems

(e.g., *ATF3*, *LECT2*, *CALR3b*, *HSPA5*, *HSPA8*, *CLDNE* and *MHC-1*), regulation of actin cytoskeleton (e.g., *ACTC1*) and glutathione metabolism (e.g., *RRM1*) were successfully validated by qRT-PCR. As shown in Fig.7, most of the qRT-PCR results agreed with the transcriptomic analysis, except for *ACTC1* (actin, alpha, cardiac muscle 1). The comparisons of gene expression changes between RNA-seq and qRT-PCR supported the reliability of the method we employed for the estimation of gene expression.

4 Discussion

4.1 DEG Analysis and Gene Expression Trends for the Stress Duration

According to clustering, the RNA-seq successfully grouped the samples under identical stress responses by gene expression profiles. Nevertheless, similar experimental treatments (light, dark or recovery) were not clustered together as expected, indicating that light and dark treatments are not the principal stress factors. Fig.3(A) identifies 521 shared DEGs in two comparisons, in spite of different light durations. In addition to the large number of shared DEGs, many functional GO terms and KEGG pathways were both enriched in two cases (Tables 3 and 4). Table 4 and Fig.8 show that osteoclast differentiation pathway was enriched in two comparisons. Previous studies reported that osteoclast differentiation plays an important role in response to hypoxic stress in

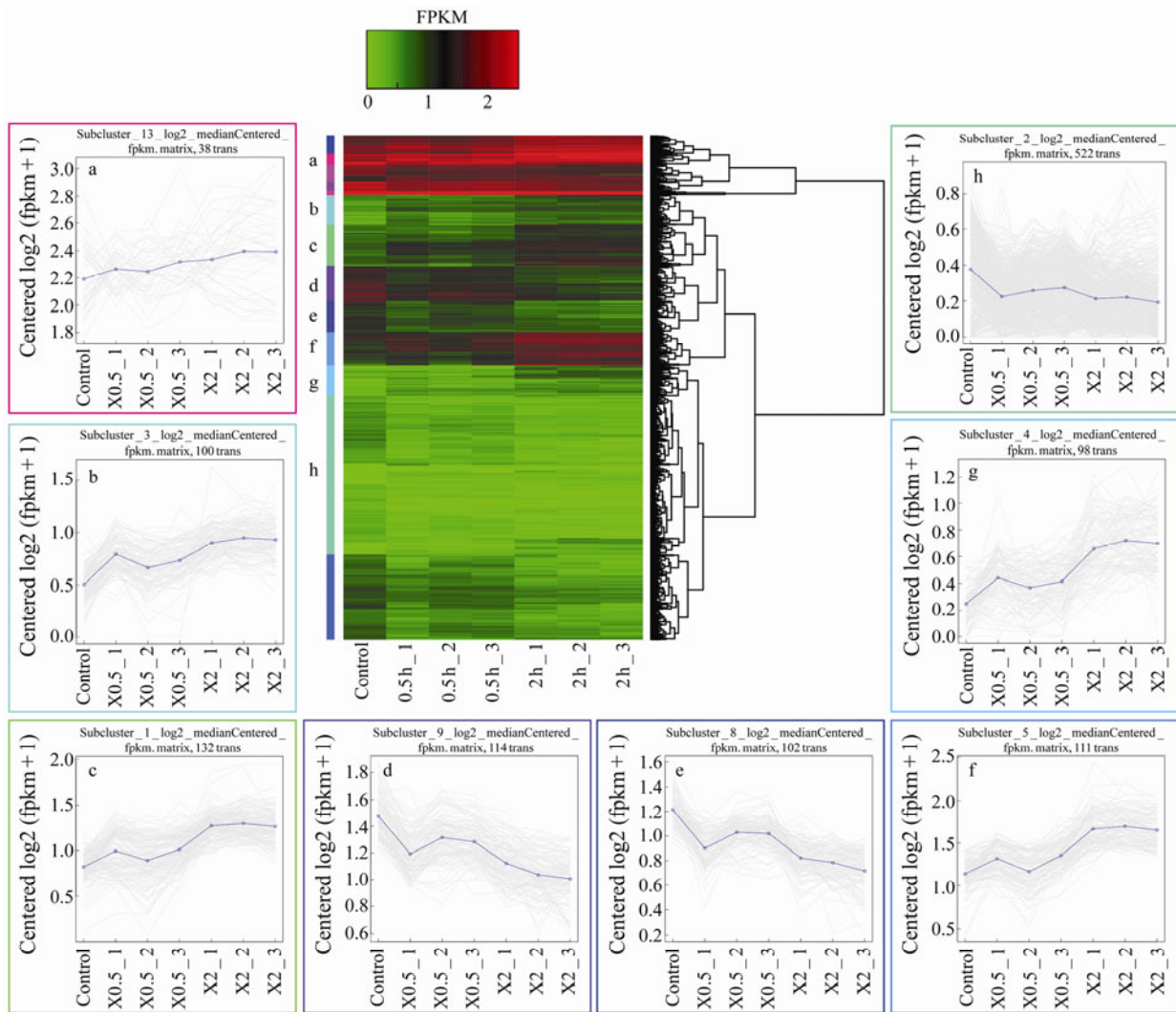


Fig.6 Heat map and subclusters expression change of experimental *L. crocea* samples. The color scheme in the heat map represents gene expression measured by FPKM. Eight clusters surrounding the heat map show the representative gene expression trends. The most significantly enriched pathway for each clusters are: (a) regulation of synaptic transmission, (b) fatty acid metabolic process, (c) response to lipid, (d) response to external stimulus, (e) oxidoreductase activity, (f) inactivation of MAPK activity, (g) intermediate filament cytoskeleton organization, and (h) mitotic cell cycle.

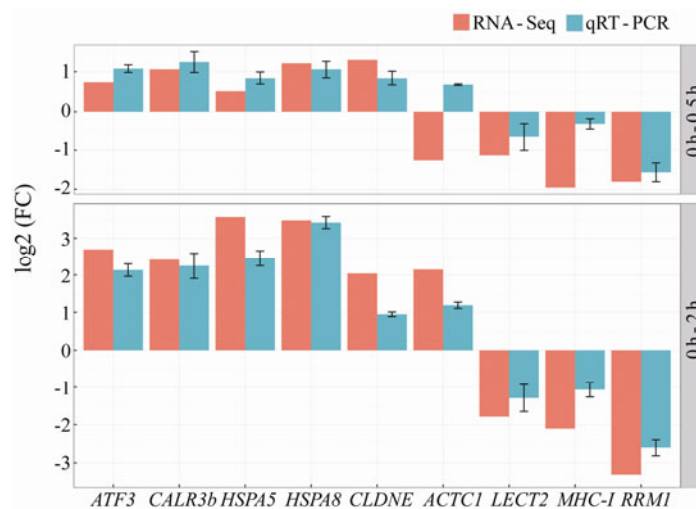


Fig.7 Comparison of relative fold changes from RNA-seq and qRT-PCR in the 0h–0.5h and 0h–2h studies. The transcript expression levels of the selected genes are normalized to that of the β -actin gene. *ATF3*: activating transcription factor 3; *CALR3b*: calreticulin 3b; *HSPA5*: heat shock 70kDa protein 5; *HSPA8*: heat shock protein 8; *CLDNE*: claudin e; *ACTC1*: actin, alpha, cardiac muscle 1; *LECT2*: leukocyte cell-derived chemotaxin 2; *MHC-1*:major histocompatibility complex I; *RRM1*: ribonucleotide reductase M1.

mice (Fukuoka *et al.*, 2005), suggesting teleost share similar molecular response to hypoxic stress in terms of osteoclast differentiation. There were more specific DEGs and enriched function in the 0 h–2 h comparison group, indicating that the molecular response of the large yellow croaker to the light duration is a continuous regulation pro-

gress. Additionally, the gene expression clusters for DEGs revealed regular increasing/decreasing gene expression trends for stress resistance (Fig. 6). The genes with identical trends may be regulated by similar genes or pathways. Therefore, the gene expression trends illuminated the fine-tuned regulation networks underlying the stress.

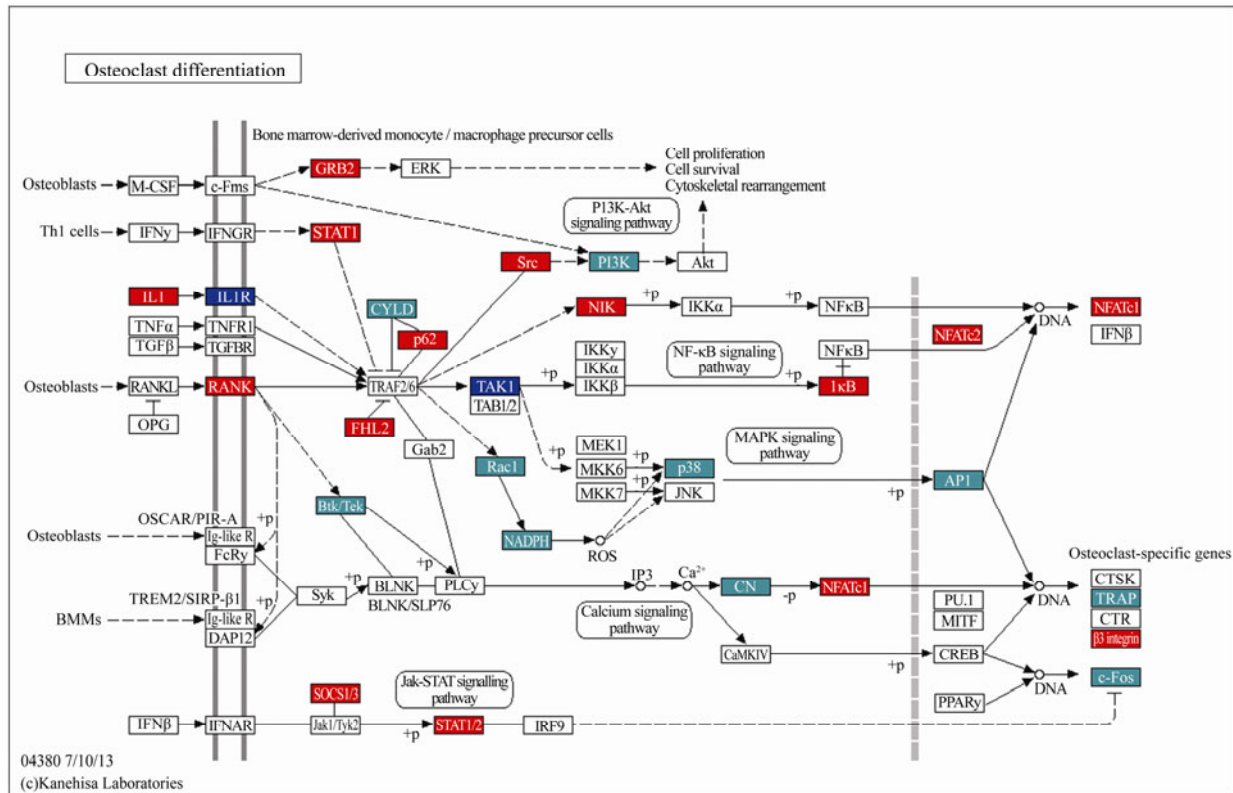


Fig. 8 DEGs list involved in osteoclast differentiation pathway (K04380). Blue, red and green color represents for specific DEGs in the 0 h–0.5 h comparison, 0 h–2 h comparison and both comparisons, respectively.

4.2 Important Biological Genes and Pathways for the Light Stress

For pathway enrichment analysis of DEGs in duration comparisons, immunity, metabolism and actin were most frequently represented categories. For immunity category, response to external biotic stimulus, leukocytes transmitting, phagosome and antigen processing and presentation subcategories were largely enriched and represented in both comparisons. Up-regulated gene of activating transcription factor 3 (*ATF3*) and down-regulated gene of leucocyte cell-derived chemotaxin-2 (*LECT2*) were involved in pathway of responding to external biotic stimulus. *ATF3* was shown to have a crucial role in the coordinate gene expression induced by eukaryotic initiation factor 2 (*eIF2*), and occurs early in response to a more diverse set of environmental stress (Jiang *et al.*, 2004). Similarly, *LECT2* was a key gene for cell growth, differentiation and autoimmune (Li *et al.*, 2008). It was involved in response pathways to external biotic stimulus. The activation of phagosome leads to rapid killing and degradation of bacteria, thus preventing escape of bacteria to the cytosol (Herskovits *et al.*, 2007). In a similar manner, MAP kinases (MAPKs) play significant roles in

the immune system by regulating key cellular events including cell migration and phagocytosis (Crean *et al.*, 2002; Huang *et al.*, 2009). It was reported in previous studies that the hypothalamic-pituitary-adrenal (HPA) axis could prevent cerebral inflammation by the suppression of *ET-1* (endothelin-1) and *ADM* (adrenomedullin) (Nadeau and Rivest, 2003; Sorrells and Sapolsky, 2007; Hayashi *et al.*, 2004; Takahashi *et al.*, 2003), and the HPA axis is mainly activated by *ET-1/ADM* and *IL-6/TNF-α* in hypoxia (Ao *et al.*, 2015). RNA-seq analysis indicated that the expression of inflammatory cytokine genes (*IL-6/TNF-α*) was significantly regulated to protect individuals from cerebral inflammatory injury. Energy metabolism and cellular differentiation were the two major subclasses of metabolism analysis. Energy metabolism related pathways such as oxoacid metabolic process and carboxylic acid metabolic process were obviously detected after 2 h duration stress. In the previous ischemic/hypoxic brain studies, energy metabolism was considered to play a key role in protecting the organs from the consequences of energy deprivation (Schurr, 2002). And a broad range of functions in energy metabolism were enriched in KEGG pathway, such as arginine and proline metabolism, fructose and mannose metabolism. This led

to a speculation that the regulation on energy metabolism would keep energy supplies under hypoxia. Prior report suggests that neuro-endocrine-immune regulatory networks help this fish avoid cerebral inflammatory injury and maintain energy balance under hypoxia stress (Ao *et al.*, 2015). Oxidoreductase activity (Fig.6e) and related genes *TRα* (hyroid hormone receptor α) were significantly down-regulated during the stress treatment, which might help to reduce cellular oxygen consumption during the process of stressing. Broad immune-relevant genes and metabolism identified in duration stress indicated a well-developed immunity system of this species responding to external stress.

In addition, DEGs identified between light and dark exhibit significant enrichments in cytoskeletal proteins and pigmentation. Cytoskeletal proteins are indispensable for mechano-transduction processes, since cytoskeletal network facilitates the translocation of signal molecules from the focal adhesion site to the cytoplasm (Shyy and Chien, 2002). The *ACTC1* (actin, alpha, cardiac muscle 1) gene expresses in strained muscle and encodes cardiac muscle alpha actin, which can function in the maintenance of cytoskeleton, cell motility and muscle contraction (Bertola *et al.*, 2008). Muscle cell development relevant gene of Myosin-7B (*MYH7B*) was involved in muscle contraction (Desjardins *et al.*, 2002). We also noticed that the developmental pigmentation (GO:0048066) and regulation of retinoic acid biosynthetic process (GO:1900052) were enriched. Thus, we speculated that the fish firstly perceived changes of light intensity using eye, then led to cytoskeleton construction induced by the skeletal muscle cell development can cause the contraction of pigment cell, and eventually promoted skin coloration changes. This can partially explain the abdominal skin coloration change from yellowish to golden yellow when they were transferred from light to dark. Further investigation was still needed to validate this speculation.

5 Conclusions

This study provided the gene expression profiles responding to the light and dark stress with two different durations. The results revealed that many genes involved in immune responses and energy metabolism, such as *ATF3*, *LECT2*, *ADM*, *IL-6/INF- α* and *TRα*, were significantly influenced by the stress durations. These genes and involved pathways are crucial to avoid cerebral inflammatory injury and to maintain energy balance of the stressed large yellow croakers. The identified DEGs related to those biological functions offer us systematic knowledge to understand gene expression trends and regulations responding to stress in *L. crocea*. Additionally, light and dark comparisons suggest that the skin coloration change is likely attributed to changes in the density of chromatophores according to DEGs annotations. The gene expression trends identified in this study will facilitate the gene network analysis in the future. In a summary, the transcriptome profile analysis would provide valuable

information for future studies on coloration change and broad stress response in teleosts.

Acknowledgements

This work was supported by grants from the National Natural Science Foundation of China (No. U1205122), Key projects of the Xiamen Southern Ocean Research Center (14GZY70NF34), the Natural Science Foundation of Fujian Province (No. 2015J05069), 'Li ShangDa' Foundation and Innovation Research Team Foundation of Jimei University (No. 2010A02). The authors thank Wanbo Li and Edna Falcis Salcedo as they revised the manuscript and gave a lot of helpful suggestions.

References

- Ao, J., Mu Y., Xiang, L., Fan, D. D., Feng, M., Zhang, S., Shi, Q., Zhu, L. Y., Li, T., and Ding, Y., 2015. Genome sequencing of the perciform fish *Larimichthys crocea* provides insights into molecular and genetic mechanisms of stress adaptation. *PLoS Genetics*, **11** (4): e1005118, DOI: 10.1371/journal.pgen.1005118.
- Bertola, L. D., Ott, E. B., Griepsma, S., Vonk, F. J., and Bagowski, C. P., 2008. Developmental expression of the alpha-skeletal actin gene. *BMC Evolutionary Biology*, **8** (1): 166.
- Blanco-Vives, B., and Sánchez-Vázquez, F. J., 2009. Synchronisation to light and feeding time of circadian rhythms of spawning and locomotor activity in zebrafish. *Physiology & Behavior*, **98** (3): 268-275.
- Crean, J. K., Finlay, D., Murphy, M., Moss, C., Godson, C., Martin, F., and Brady, H. R., 2002. The role of p42/44 MAPK and protein kinase B in connective tissue growth factor induced extracellular matrix protein production, cell migration, and actin cytoskeletal rearrangement in human mesangial cells. *Journal of Biological Chemistry*, **277** (46): 44187-44194, DOI: 10.1074/jbc.M203715200.
- Desjardins, P. R., Burkman, J. M., Shrager, J. B., Allmond, L. A., and Stedman, H. H., 2002. Evolutionary implications of three novel members of the human sarcomeric myosin heavy chain gene family. *Molecular Biology and Evolution*, **19** (4): 375-393.
- Dong, L. S., Xiao, S. J., Wang, Q. R., and Wang, Z. Y., 2016. Comparative analysis of the GBLUP, emBayesB, and GWAS algorithms to predict genetic values in large yellow croaker (*Larimichthys crocea*). *BMC Genomics*, **17** (1): 460, DOI: 10.1186/s12864-016-2756-5.
- Fu, X., Sun, Y., Wang, J., Xing, Q., Zou, J., Li, R., Wang, Z., Wang, S., Hu, X., Zhang, L., and Bao, Z., 2014. Sequencing-based gene network analysis provides a core set of gene resource for understanding thermal adaptation in Zhikong scallop *Chlamys farreri*. *Molecular Ecology Resources*, **14** (1): 184-198, DOI: 10.1111/1755-0998.12169.
- Fukuoka, H., Aoyama, M., Miyazawa, K., Asai, K., and Goto, S., 2005. Hypoxic stress enhances osteoclast differentiation via increasing IGF2 production by non-osteoclastic cells. *Biochemical and Biophysical Research Communications*, **328** (4): 885-894, DOI: 10.1016/j.bbrc.2005.01.042.
- Gu, X., and Xu, Z., 2011. Effect of hypoxia on the blood of large yellow croaker (*Pseudosciaena crocea*). *Chinese Journal of Oceanology and Limnology*, **29**: 524-530, DOI: 10.1007/s00343-011-0109-4.

- Hayashi, R., Wada, H., Ito, K., and Adcock, I. M., 2004. Effects of glucocorticoids on gene transcription. *European Journal of Pharmacology*, **500** (1): 51-62, DOI: 10.1016/j.ejphar.2004.07.011.
- Herskovits, A. A., Auerbuch, V., and Portnoy, D. A., 2007. Bacterial ligands generated in a phagosome are targets of the cytosolic innate immune system. *PLoS Pathogens*, **3** (3): e51, DOI: 10.1371/journal.ppat.0030051.
- Hooper, J. E., 2014. A survey of software for genome-wide discovery of differential splicing in RNA-Seq data. *Human Genomics*, **8** (1): 1, DOI: 10.1186/1479-7364-8-3.
- Huang, G., Shi, L. Z., and Chi, H., 2009. Regulation of JNK and p38 MAPK in the immune system: Signal integration, propagation and termination. *Cytokine*, **48** (3): 161-169, DOI: 10.1016/j.cyt.2009.08.002.
- Jiang, H. Y., Wek, S. A., McGrath, B. C., Lu, D., Hai, T., Harding, H. P., Wang, X., Ron, D., Cavener, D. R., and Wek, R. C., 2004. Activating transcription factor 3 is integral to the eukaryotic initiation factor 2 kinase stress response. *Molecular and Cellular Biology*, **24** (3): 1365-1377, DOI: 10.1128/MCB.24.3.1365-1377.
- Larsen, P. F., Nielsen, E. E., Meier, K., Olsvik, P. A., Hansen, M. M., and Loeschcke, V., 2012. Differences in salinity tolerance and gene expression between two populations of atlantic cod (*Gadus morhua*) in response to salinity stress. *Biochemical Genetics*, **50** (5-6): 454-466, DOI: 10.1007/s10528-011-9490-0.
- Li, M. Y., Chen, J., and Shi, Y. H., 2008. Molecular cloning of leucocyte cell-derived chemotaxin-2 gene in croceine croaker (*Pseudosciaena crocea*). *Fish & Shellfish Immunology*, **24** (2): 252-256, DOI: 10.1016/j.fsi.2007.09.003.
- Liu, X., Zhao, G., Cai, M., and Wang, Z., 2013. Estimated genetic parameters for growth-related traits in large yellow croaker *Larimichthys crocea* using microsatellites to assign parentage. *Journal of Fish Biology*, **82** (1): 34-41, DOI: 10.1111/j.1095-8649.2012.03472.x.
- Liu, Y., Cao, M., Zhang, M., Hu, J., Zhang, Y., Zhang, L., and Liu, G., 2014. Purification, characterization and immunoreactivity of β -component, a major allergen from the roe of large yellow croaker (*Pseudosciaena crocea*). *Food and Chemical Toxicology*, **72**: 111-121, DOI: 10.1016/j.fct.2014.07.015.
- Mu, Y., Ding, F., Cui, P., Ao, J., Hu, S., and Chen, X., 2010. Transcriptome and expression profiling analysis revealed changes of multiple signaling pathways involved in immunity in the large yellow croaker during *Aeromonas hydrophila* infection. *BMC Genomics*, **11** (1): 1, DOI: 10.1186/1471-2164-11-506.
- Nadeau, S., and Rivest, S., 2003. Glucocorticoids play a fundamental role in protecting the brain during innate immune response. *The Journal of Neuroscience*, **23** (13): 5536-5544.
- Robinson, M. D., McCarthy, D. J., and Smyth, G. K., 2010. edgeR: A bioconductor package for differential expression analysis of digital gene expression data. *Bioinformatics*, **26** (1): 139-140, DOI: 10.1093/bioinformatics/btp616.
- Schartl, M., Walter, R. B., Shen, Y., Garcia, T., Catchen, J., Amores, A., Braasch, I., Chalopin, D., Volff, J. N., Lesch, K. P., Bisazza, A., Minx, P., Hillier, L., Wilson, R. K., Fuerstenberg, S., Boore, J., Searle, S., Postlethwait, J. H., and Warren, W. C., 2013. The genome of the platyfish, *Xiphophorus maculatus*, provides insights into evolutionary adaptation and several complex traits. *Nature Genetics*, **45** (5): 567-572, DOI: 10.1038/ng.2604.
- Schurr, A., 2002. Energy metabolism, stress hormones and neural recovery from cerebral ischemia/hypoxia. *Neurochemistry International*, **41** (1): 1-8, DOI: 10.1016/S0197-0186(01)00142-5.
- Shyy, J. Y., and Chien, S., 2002. Role of integrins in endothelial mechanosensing of shear stress. *Circulation Research*, **91** (9): 769-775, DOI: 10.1161/01.RES.0000038487.19924.18.
- Smith, S., Bernatchez, L., and Beheregaray, L. B., 2013. RNA-seq analysis reveals extensive transcriptional plasticity to temperature stress in a freshwater fish species. *BMC Genomics*, **14** (1): 1, DOI: 10.1186/1471-2164-14-375.
- Sorrells, S. F., and Sapolsky, R. M., 2007. An inflammatory review of glucocorticoid actions in the CNS. *Brain Behavior and Immunity*, **21** (3): 259-272, DOI: 10.1016/j.bbi.2006.11.006.
- Su, Y., Zhang, C., and Wang, J., 2007. *Breeding and Farming of Pseudosciaena crocea*. Ocean Press, Beijing, 329pp.
- Takahashi, K., Udono-Fujimori, R., Totsune, K., Murakami, O., and Shibahara, S., 2003. Suppression of cytokine-induced expression of adrenomedullin and endothelin-1 by dexamethasone in T98G human glioblastoma cells. *Peptides*, **24** (7): 1053-1062, DOI: 10.1016/S0196-9781(03)00181-5.
- Trapnell, C., Hendrickson, D. G., Sauvageau, M., Goff, L., Rinn, J. L., and Pachter, L., 2013. Differential analysis of gene regulation at transcript resolution with RNA-seq. *Nature Biotechnology*, **31** (1): 46-53, DOI: 10.1038/nbt.2450.
- Trapnell, C., Roberts, A., Goff, L., Pertea, G., Kim, D., Kelley, D. R., Pimentel, H., Salzberg, S. L., Rinn, J. L., and Pachter, L., 2012. Differential gene and transcript expression analysis of RNA-seq experiments with TopHat and Cufflinks. *Nature Protocols*, **7** (3): 562-578, DOI: 10.1038/nprot.2012.016.
- Tu, Q., Cameron, R. A., Worley, K. C., Gibbs, R. A., and Davidson, E. H., 2012. Gene structure in the sea urchin *Strongylocentrotus purpuratus* based on transcriptome analysis. *Genome Research*, **22** (10): 2079-2087, DOI: 10.1101/gr.139170.112.
- Upton, G. J., 1992. Fisher's exact test. *Journal of the Royal Statistical Society Series A (Statistics in Society)*, **155** (3): 395-402, DOI: 10.2307/2982890.
- Xiao, S., Li, J., Ma, F., Xu, S., Chen, W., and Wang, Z., 2015. Rapid construction of genome map for large yellow croaker (*Larimichthys crocea*) by the whole-genome mapping in BioNano Genomics Irys system. *BMC Genomics*, **16** (1): 670, DOI: 10.1186/s12864-015-1871-z.
- Yang, X., Liu, D., Liu, F., Wu, J., Zou, J., Xiao, X., Zhao, F., and Zhu, B., 2013. HTQC: A fast quality control toolkit for Illumina sequencing data. *BMC Bioinformatics*, **14** (1): 1, DOI: 10.1186/1471-2105-14-33.
- Ye, H., Liu, Y., Liu, X., Wang, X., and Wang, Z., 2014. Genetic mapping and QTL analysis of growth traits in the large yellow croaker *Larimichthys crocea*. *Marine Biotechnology*, **16** (6): 729-738, DOI: 10.1007/s10126-014-9590-z.
- Ye, J., Fang, L., Zheng, H., Zhang, Y., Chen, J., Zhang, Z., Wang, J., Li, S., Li, R., Bolund, L., and Wang, J., 2006. WEGO: A web tool for plotting GO annotations. *Nucleic Acids Research*, **34** (suppl 2): 293-297, DOI: 10.1093/nar/gkl031.
- Zhou, Y., Yan, X., Xu, S., Zhu, P., He, X., and Liu, J., 2011. Family structure and phylogenetic analysis of odorant receptor genes in the large yellow croaker (*Larimichthys crocea*). *BMC Evolutionary Biology*, **11** (1): 237, DOI: 10.1186/1471-2148-11-237.

(Edited by Qiu Yantao)